Liquid–gas interface under hydrostatic pressure

A. Gajewski
Bialystok University of Technology, Faculty of Civil Engineering and Environmental Engineering, Department of Heat Engineering, Poland

Abstract

The surface-tension forces and the pressure force at a gas–liquid interface were balanced. This was done at a differential control surface under hydrostatic pressure. As a result, three quadratic and two linear equations were derived representing the conditions for equilibrium at the interface. These equations have eight roots describing eleven different equilibrium states. The most important is the Young-Laplace formula under hydrostatic pressure which is denoted in the spherical coordinate system. Hence, it is a quadratic equation. The first root of this equation describes a pendant drop, drop or bubble, while the second one circumscribes a sessile drop. There are two solutions for the uniform pressure, where one of them is the Young-Laplace formula. It is concluded that the surface existence depends on the pressure difference between both bulk phases. A plane is formed when the surface-tension forces equilibrate themselves. Under uniform pressure the interface is a sphere and its other shapes need a pressure gradient. To form a drop or a bubble the pressure difference must be higher than its border value. A sessile drop exists if the gauge pressure is negative, while a pendant drop requires a positive value. A comparison with experimental results is done for the bubble.
Keywords: Young-Laplace equation in spherical coordinates, static equilibrium, drop, bubble.

1 Introduction

To describe the force balance on the liquid–gas interface, the Young-Laplace equation is usually applied. The equation must be solved for each point separately. Hence, it is computationally difficult to balance the surface-tension

WIT Transactions on Engineering Sciences, Vol 74, © 2012 WIT Press
www.witpress.com, ISSN 1743-3533 (on-line)
doi:10.2495/AFM120231

and hydrodynamic forces on a differential surface or volume. The Young-Laplace equation was derived from work involving the expansion of a soap-bubble surface. The same formula can be also applied as a condition of static equilibrium because the surface tension is considered simultaneously as a surface-tension force per unit length and, following Tolman [1], either as the quotient of the energy change with the change in surface area at constant entropy, constant composition and constant volumes for the two phases (measured at the surface of tension) or as the rate of free energy change with the change in surface area at constant temperature, constant composition and constant volumes. The theory of wetting phenomena on curved surfaces has been developed to date by the derivation of formulas or theorems originating from an "energetic" definition and their application in force balances. Hence, this solution is limited to one scalar equation. Because a force may have three components, this equation may not be applied as a condition for equilibrium in the case of an unsymmetrical shape, nor can the shape of the surface be described using only the force balance due to the lack of the corresponding equations along the tangents to the surface directions.

The main goal of the current work is to develop a wetting theory of curved gas-liquid interfacial surfaces beginning directly from the surface tension defined as the unit force. This was expected to yield two equations of force balance for the symmetric shapes for the droplet or bubble under hydrostatic pressure.

2 Mathematical model

The topic of discussion here is the prediction of the shape of the liquid–gas interface under hydrostatic pressure. To do it, the forces applied on the surface at rest are balanced. As surface forces shape the surface, they should be balanced at the surface. While the fixed coordinate system is used, the hydrostatic pressure creates a changing radius of curvature. Therefore, the surface with a varying radius along the depth of the liquid must be described.

The surface presented in fig. 1 is defined in the spherical parameterisation in which the radial distance changes along the θ coordinate:

$$f(\theta,\varphi) = \left(r(\theta)\sin\theta\cos\varphi, r(\theta)\sin\theta\sin\varphi, r(\theta)\cos\theta\right) \tag{1}$$

The versors of the surface-coordinate system are

$$\vec{\delta}_\theta = \cos(\theta-\omega)\cos\varphi\vec{i} + \cos(\theta-\omega)\sin\varphi\vec{j} - \sin(\theta-\omega)\vec{k} \tag{2}$$

$$\vec{\delta}_\varphi = -\sin\varphi\vec{i} + \cos\varphi\vec{j} \tag{3}$$

where ω is defined in fig. 3.

Moving along the tangential vector, the surface curves in the direction of the movement. The curvature is described by the unit vector perpendicular to the surface. It arises from the structure of the surface, which is a two-dimensional object existing in three-dimensional space. Taking the above into account, it is necessary to define the normal unit vector:

$$\vec{\delta}_n = \sin(\theta-\omega)\cos\varphi\vec{i} + \sin(\theta-\omega)\sin\varphi\vec{j} + \cos(\theta-\omega)\vec{k} \tag{4}$$

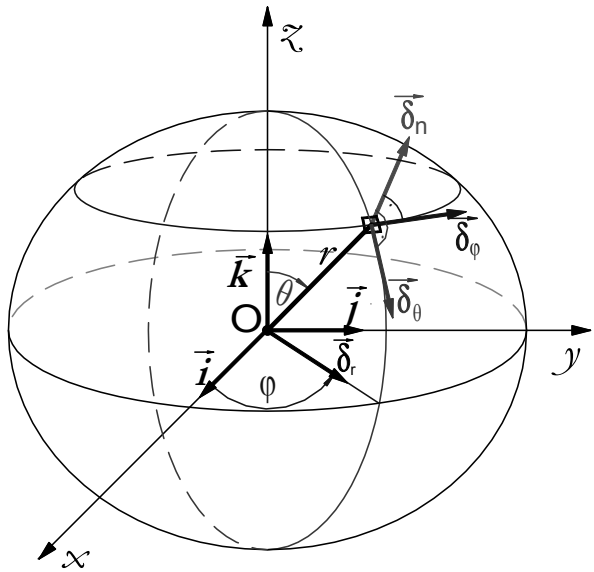

Figure 1: The assumed surface coordinates and the versors.

2.1 The force system

No matter how small, a fluid is a substance that deforms continuously under the application of tangential stress. In the considered case, the shear stresses equal zero. Therefore, only the normal stresses are sustained. As a result, the resultant force acting on the surface is normal to the surface. The resultant pressure force that tends to expand the surface, acts in the centre of the area. Because the force system has to satisfy Newton's third law, the directions and senses of the resultant surface forces preventing expansion must be oriented out from the surface. However, the components of the resultant surface-tension forces must be applied at the boundary arc of the surface, and these are tangential to the surface.

The force system is shown in fig. 2. In this case, the resultant pressure force is the active force. Therefore, the resultant of the tangential surface forces is the reactive force. A differential surface element is defined using two arcs with radii r and $r\sin\theta$ (cf. fig. 2). Therefore, this surface is a curvilinear rectangle (fig. 1 and fig. 2). Hence, we have four infinitesimal surface-tension forces (fig. 2). As a result, we obtain two resultants, one each of each pair of these forces. These resultants equilibrate the infinitesimal pressure force.

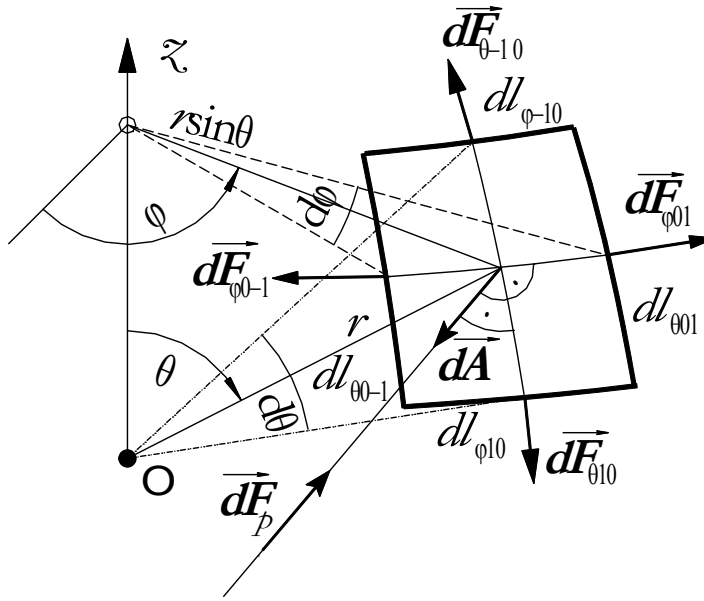

Figure 2: The force system for an infinitesimal element.

The pressure force is expressed by the formula

$$d\vec{F}_p = -p d\vec{A} = p\frac{r^2 \sin\theta d\theta d\varphi}{\cos\omega}\vec{\delta}_{n00} \tag{5}$$

The surface tension forces in the φ component are presented

$$d\vec{F}_{\varphi 01} = \left(\sigma r d\theta / \cos\omega\right)\vec{\delta}_{\varphi 01} \tag{6}$$

$$d\vec{F}_{\varphi 0-1} = \left(-\sigma r d\theta / \cos\omega\right)\vec{\delta}_{\varphi 0-1} \tag{7}$$

Next, the components in the θ direction are obtained:

$$d\vec{F}_{\theta 10} = \sigma\left(r + dr/2\right)\sin\left(\theta + d\theta/2\right)d\varphi\vec{\delta}_{\theta 10} \quad , \tag{8}$$

$$d\vec{F}_{\theta -10} = -\sigma\left(r - dr/2\right)\sin\left(\theta - d\theta/2\right)d\varphi\vec{\delta}_{\theta -10} \quad . \tag{9}$$

The resultant force in the θ direction is:

$$d\vec{F}_\theta = \sigma\left(r \sin d\theta \cos\theta + dr \sin\theta \cos^2\frac{d\theta}{2}\right)d\varphi\vec{\delta}_{\theta 00} - \sigma r \sin\theta \sin d\theta d\varphi\vec{\delta}_{n00} \tag{10}$$

and in the φ direction:

$$d\vec{F}_\varphi = -2\sigma\frac{rd\theta}{\cos\omega}\cos\theta \sin\frac{d\varphi}{2}\vec{\delta}_{\theta 00} - 2\sigma\frac{rd\theta}{\cos\omega}\sin\theta \sin\frac{d\varphi}{2}\vec{\delta}_{n00} \tag{11}$$

The system of the resultant forces and the cross section of the investigated surface are showed in fig. 3. Hydrostatic pressure is calculated as follows:

$$p = \rho g\left(r_0 - r\cos\theta\right) \quad . \tag{12}$$

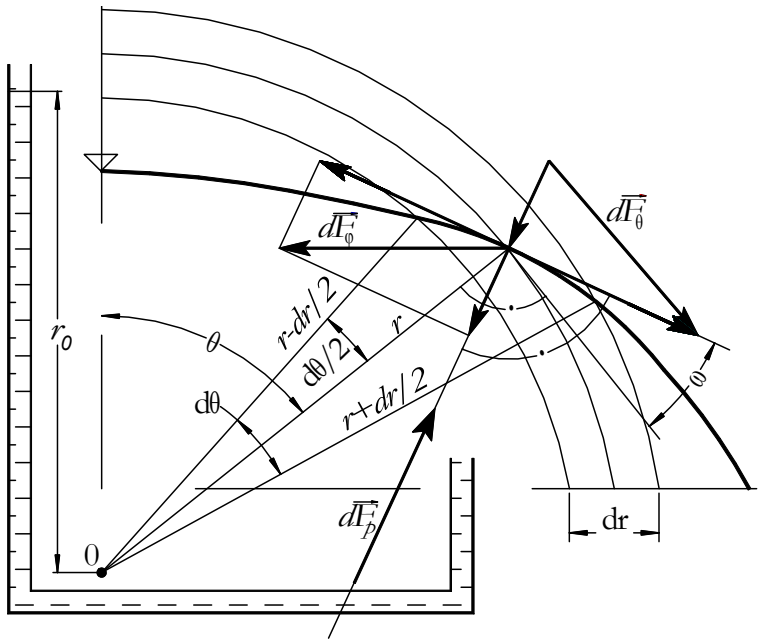

Figure 3: The force system resolved into meridian and normal directions.

2.2 The force balance

The resultant surface tension forces and pressure force are balanced. Respectively, their components along the meridian and normal directions to the surface must equal zero. First we obtain the force balance in tangential direction:

$$1+\frac{dr}{rd\theta}\tan\theta=\sqrt{1+\left(dr/rd\theta\right)^2} \tag{13}$$

and the balance of the forces in the normal direction:

$$\frac{dr}{d\theta}=r\sqrt{\frac{1}{\left(\frac{\rho g r\left(r_0-r\cos\theta\right)}{\sigma}-1\right)^2}-1} \tag{14}$$

Substituting the relationship

$$r^+=r/\sqrt{\sigma/\rho g} \tag{15}$$

into Eqs. (13) and (14), we obtain a system of dimensionless equations as follows:

$$\begin{cases}\dfrac{dr^+}{r^+d\theta}\left[\dfrac{dr^+}{r^+d\theta}\left(\tan^2\theta-1\right)+2\tan\theta\right]=0\\ \dfrac{dr^+}{r^+d\theta}-\sqrt{\dfrac{1}{\left(r^+\left(r_o^+-r^+\cos\theta\right)-1\right)^2}-1}=0\end{cases} \tag{16}$$

for which the solution is the product of the left sides of the five equations:

$$r^+\left(r_o^+ - r^+ \cos\theta\right) - 2 = 0 \tag{17}$$

$$r^+ = 0 \tag{18}$$

$$r_o^+ - r^+ \cos\theta = 0 \tag{19}$$

$$r^+\left(r_o^+ - r^+ \cos\theta\right) - 2\sin^2\theta = 0 \tag{20}$$

$$r^+\left(r_o^+ - r^+ \cos\theta\right) - 2\cos^2\theta = 0 \tag{21}$$

These equations can be expressed in dimensional form as

$$\rho g\left(r_0 - r\cos\theta\right) = 2\sigma/r \tag{22}$$

$$r = 0 \tag{23}$$

$$\rho g\left(r_0 - r\cos\theta\right) = 0 \tag{24}$$

$$\rho g\left(r_0 - r\cos\theta\right) = 2\sigma\sin^2\theta/r \tag{25}$$

$$\rho g\left(r_0 - r\cos\theta\right) = 2\sigma\cos^2\theta/r \tag{26}$$

Formulas (17) and (22) are the Young-Laplace equation for the hydrostatic pressure written in spherical coordinates. These formulas can be solved as a quadratic equation with r as the variable. Hence, the shape of the surface can be found easily.

In contrast, their solution in the Cartesian coordinate system, in which the double surface tension is divided by the radius of curvature, requires the solution of a second-order differential equation. It can be concluded that the surface can exist if the resultant surface-tension force equals zero (cf. Eq. (24)), but it cannot be formed if the hydrostatic pressure is equal to zero. The last conclusion arises from the analysis of Eqs. (22), (24), (25) and (26) and is expressed implicitly by Eq. (23).

2.3 The shapes of the interfaces

As the shapes of the liquid–gas interfaces are presented by the solutions of Eqs. (17)–(21), we can distinguish four kinds of surface equilibrium. The first is described the Young-Laplace formula, i.e., Eq. (17). The second is the flat surface, expressed by Eq. (19), with a lack of a surface as its particular case (cf. Eq. (18)). The third and fourth kinds of equilibria have not been connected with any real situation so far. Therefore, they can be only the solutions of the force balance without any physical meaning.

Although the analysis is made in the surface-coordinate system, the graphs are plotted in Cartesian coordinates:

$$x^+ = r^+ \sin\theta \tag{27}$$

$$z^+ = r^+ \cos\theta \tag{28}$$

where the variables are defined in fig. 1. Because these solutions have axisymmetric shapes, they are plotted as cross-sections in the x^+z^+ plane.

2.3.1 The Young-Laplace equation

The solution of Eq. (17), i.e., the Young-Laplace formula with hydrostatic pressure in spherical coordinates, has two roots:

$$r_1^+ = \frac{r_o^+ - \sqrt{r_o^{+2} - 8\cos\theta}}{2\cos\theta} \tag{29}$$

$$r_2^+ = \frac{r_o^+ + \sqrt{r_o^{+2} - 8\cos\theta}}{2\cos\theta} \tag{30}$$

Because these solutions have discontinuities at $\theta = \pi/2$, the limits of the functions at this point must be calculated. To do so, we represent the square roots in Eqs. (29) and (30) as Taylor series. If $r_0^+ \Big/ \sqrt{r_0^{+2}} = 1$, the limits of the roots r_1^+ and r_2^+ are calculated as follows:

$$\lim_{\theta \to \pi/2} r_1^+ = \frac{2}{r_o^+} \tag{31}$$

$$\lim_{\theta \to \pi/2} r_2^+ = -\infty \tag{32}$$

If $r_0^+ \Big/ \sqrt{r_0^{+2}} = -1$, these limits are presented below:

$$\lim_{\theta \to \pi/2} r_1^+ = \infty, \tag{33}$$

$$\lim_{\theta \to \pi/2} r_2^+ = \frac{2}{r_o^+} \tag{34}$$

Hence, in the case of a positive hydraulic head, r_0^+, the root r_1^+ is a continuous function. If the hydraulic head has a negative value, the solution for r_2^+ has no discontinuity. We can summarise that the hydraulic head is the asymptote for some solutions. Note that r_1^+ and r_2^+ can generally be complex numbers. To return a real number for the square root over the interval $0 \le \theta \le \pi$, $\left|r_0^+\right|$ cannot be less than $2\sqrt{2}$. Over the domain $\pi/2 < \theta \le \pi$, cosine θ is less than zero, and so the discriminant has a positive value. The solutions of these equations for this positive border values are presented in fig. 4. The graphs for r_1^+ and for r_2^+ over the interval $0 \le \theta < \pi/2$ show the shapes of the interfaces when the pressure inside is higher than their surroundings. The plots for r_2^+ over the interval $\pi/2 < \theta \le \pi$ present the surface limited in volume with internal pressure lower than the surroundings.

In the case of higher gauge pressure, the drop has no tangent point with the upper layer, but its shape is almost spherical because the vertical diameter is slightly longer than the horizontal one. These diameters will be equal if $r_0^+ = 55.2$, and so the drop will then be a sphere.

The sample solution for $0 < r_0^+ < 2\sqrt{2}$ is presented in fig. 4b). The intervals in which the real roots of eqs. (29) and (30) can be found are noted in this figure. The results for r_1^+ model the case of a pendant drop that is still connected to the solid phase. We can conclude that the drop will form if the dimensionless gauge-pressure value reaches $2\sqrt{2}$. Although gaps in the plots are observed for r_2^+ in

the domain $0 \le \theta < \pi/2$, this does not indicate a lack of the surface at the gap period in this case; rather, it only means the lack of a state of the equilibrium for the surface with the assumed force system. The surface could thus accelerate, or other forces could be introduced to the analysis. A different situation is observed in the interval $\pi/2 < \theta \le \pi$. Because cosine θ is less than zero here, the discriminant in Eq. (30) is a positive value. Thus, there is no gap for r_2^+ within this interval.

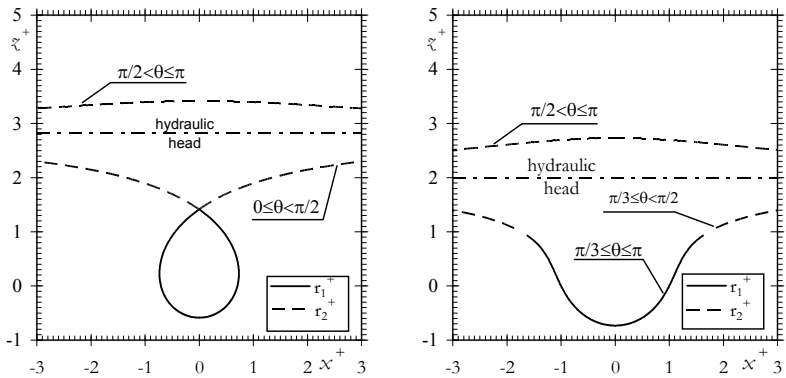

Figure 4: The plots of eqs. (29) and (30) for: a) $r_0^+ = 2\sqrt{2}$, b) $r_0^+ = 2$.

The plots for $-2\sqrt{2} < r_0^+ < 0$ are the mirror image of the plots for their modulus values. There occurs the shift between solutions for Eqs. (29) and (30). The second root describes the sessile drop well. Therefore, the plots for $r_0^+ = -2$ are the mirror image of the plots in fig. 4b), where the hydraulic head line is the axis of symmetry.

2.3.2 The flat surface and the lack of surface

The flat surface is the solution of Eq. (19):

$$r_4^+ = \frac{r_o^+}{\cos\theta} \tag{35}$$

The height of the surface or the depth of the liquid is equal to hydraulic head, r_0^+ . As the right side of Eq. (19) is zero, there is no resultant surface-tension force. However, this does not mean that these forces are not present but rather that the surface-tension forces achieve equilibrium on the plane and only their resultant does not exist.

The most extreme state is the lack of a surface if the hydraulic head equals zero, which is expressed by Eq. (20). This is an important finding of this work. The surface can exist if the surface-tension forces balance each other, but the surface cannot be shaped if there is no pressure difference between two sides of the surface (i.e., between the two bulk phases). This conclusion is confirmed by

the limit of the function calculated by Eq. (32). A liquid–gas surface will not reach the level of the hydraulic head if the surface-tension forces do not achieve equilibrium. These situations are presented in figs. 4, 5.

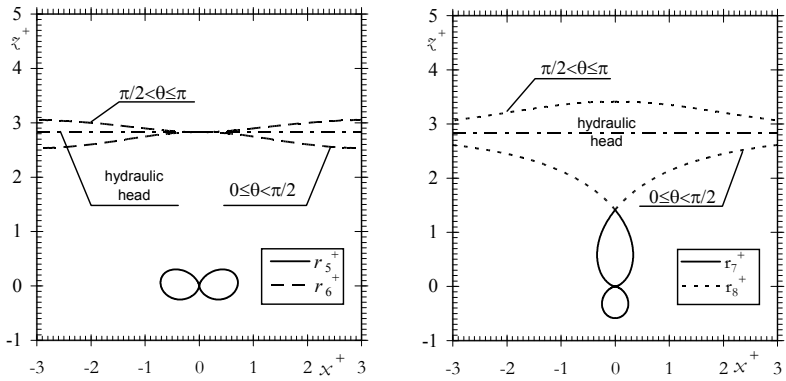

a) b)

Figure 5: a) The graphs of Eqs. (36) and (37) for $r_0^+ = 2\sqrt{2}$, b) The graphs of Eqs. (38) and (39) for $r_0^+ = 2\sqrt{2}$.

2.3.3 The third kind of equilibrium state

This solution has not been connected with any experimental observations so far, and its properties have not been described in detail.

The third equilibrium state, defined by Eq. (20), has two roots:

$$r_5^+ = \frac{r_o^+ - \sqrt{r_o^{+2} - 8\sin^2\theta\cos\theta}}{2\cos\theta} \tag{36}$$

$$r_6^+ = \frac{r_o^+ + \sqrt{r_o^{+2} - 8\sin^2\theta\cos\theta}}{2\cos\theta} \tag{37}$$

The graphs of Eq. (36), plotted in fig. 5a) have shapes similar to a horn torus. The plots of Eq. (37) are tangent to the line of the hydraulic head because sine θ for $\theta = 0$ in Eq. (20) is equal to zero. For that reason, this equation is decomposed into two: (18) and (19) (i.e., the lack of a surface and a flat surface, respectively) in this point. The solution for the plane is plotted in fig. 5a) at $\theta = 0$, which makes this solution different from the cases described in Sections 2.3.1 and 2.3.4. The depth of the lower layer (i.e., the difference between the hydraulic head and the vertical coordinate of the lower surface) is tangent to the upper plate (the solution for $0 \le \theta < \pi/2$), and it increases up to its maximum value (for $\theta = 0.9553$) then approaches the hydraulic-head line. The height of the upper layer (the solution for $\pi/2 < \theta \le \pi$) rises from 0 (for $\theta = \pi$) to its maximum (for $\theta = 2.186$) and then approaches the hydraulic-head line.

2.3.4 The fourth kind of equilibrium state

The fourth equilibrium state, given by Eq. (21), has two roots:

$$r_7^+ = \frac{r_o^+ - \sqrt{r_o^{+2} - 8\cos^3\theta}}{2\cos\theta} \tag{38}$$

$$r_8^+ = \frac{r_o^+ + \sqrt{r_o^{+2} - 8\cos^3\theta}}{2\cos\theta} \tag{39}$$

The seventh root of the general force balance given by Eq. (38) has the shape of a thin drop suspended within another one, cf. fig. 5b). The upper layer (the solution for $\pi/2 < \theta \le \pi$) is largest for $\theta = 0$, and then it decreases and approaches the hydraulic-head line. The lower layer (the solution for $0 \le \theta < \pi/2$ is deepest for $\theta = 0$, and it monotonically approaches the hydraulic-head line.

2.3.5 Surface under uniform pressure

Eq. (14) under uniform pressure takes the form

$$\frac{dr}{d\theta} = r\sqrt{\frac{1}{\left(\frac{pr}{\sigma} - 1\right)^2} - 1}\ , \tag{40}$$

while eq. (13) does not change. There are two solutions of eqs. (13) and (40):

$$p = \frac{2\sigma}{r}\ , \tag{41}$$

$$p = \frac{2\sigma}{r}\cos^2\theta \quad . \tag{42}$$

Formula (41) is well known Young-Laplace equation and describes bubble under uniform pressure that shape is spherical. Although, it is common known result, for the first time this shape was derived from the complete force balance directly. Eq. (42) seems to be only mathematical solution that has not been observed experimentally, which cross-section is two equal bubbles where second bubble is attached under the first one.

3 Summary and discussion

It was proven that it is possible to obtain a complete system of equations for the static equilibrium of a surface under hydrostatic pressure for all fluids that do not sustain shear stresses when at rest. To predict the shape of this surface, a new differential surface with a varying radial distance along the meridian direction was defined. The pressure force and surface-tension forces were balanced on this surface. In the method presented herein, it was possible to balance the surface forces and the surface-tension forces on the control surface. This had not previously been possible, and it represents the major finding of this work. As a result, a system of two equations was obtained: one each in the radial and tangential directions. Their solutions were decomposed into three quadratic and two linear equations with eight roots. Due to the existence of discontinuities, they can describe eleven different situations. The first solution is the Young-

Laplace equation with the interface under hydrostatic pressure. To obtain the results in the traditional way, a second-order differential equation must be solved. In the achieved method, a simple quadratic equation is instead solved, which makes the calculations quite simple. The linear solutions are the flat surface and the lack of a surface. Although they are both trivial, their presence proves the generality of the developed model. Furthermore, two new solutions were obtained that seem to be unconnected with any physical situation.

3.1 Conclusions

We drew the following conclusions for a surface under pressure and surface-tension forces only:

- A surface under uniform pressure is a sphere.
- A plane is formed if the surface-tension forces equilibrate themselves.
- Other shapes occur if a pressure gradient exists and the surface-tension forces equilibrate pressure force.
- A surface cannot exist without a pressure difference across both of its sides.
- The pressure forces are the active forces, whereas the surface-tension forces are the reactive forces, which only act to curve the surface.
- To form a closed interface (e.g., a drop or a bubble), the interior pressure cannot be less than its border value; i.e., the modulus of the hydraulic head must be a factor of $2\sqrt{2}$ or more times higher than the capillary constant.

Acknowledgement

This scientific research was financed from the resources of the National Centre for Science.

References

[1] R.C. Tolman, Consideration of the Gibbs Theory of Surface Tension, The Journal of Chemical Physics, Vol. 16, No. 8, 1948, 758-774.
[2] Thoroddsen S.T., Etoh T.G., Takehara K., High-Speed Imaging of Drops and Bubbles, Annu. Rev. Fluid Mech. 2008, 40:257-85.